Research on the Use of Nano-starch Crystals as Rheological Performance Regulators in Drilling Fluids

Guowei Zhou *, Xin Zhang , Weijun Yan , Zhengsong Qiu

Posted Date: 22 April 2025

doi: 10.20944/preprints202504.1790.v1

Keywords: drilling fluids; thermal stability; rheological property regulator; nanostarch crystals; thixotropy

 doi:10.20944/preprints202504.1790.v1

Article

Research on the Use of Nano-Starch Crystals as Rheological Performance Regulators in Drilling Fluids

Guowei Zhou [1], Xin Zhang [1] Weijun Yan [1], Zhengsong Qiu [2]

[1] CNPC Greatwall Drilling Company. 101 Anli Road, Chaoyang District, Peking 10020, China
[2] China University of Petroleum (East China). No.66 Changjiang East Road, Huangdao District, Qingdao, Shandong Province 266000, China
* Correspondence: zhgw1027@163.com

Abstract: With the depletion of shallow hydrocarbon reservoirs, deep petroleum exploration is emerging as a technical focus in the industry, where elevated formation temperatures impose stringent requirements for drilling fluid thermal stability. Concurrently, extended-reach horizontal well (ERHW) technology is widely adopted in offshore development to enhance single-well productivity, demanding drilling fluids that have superior cuttings transport efficiency and environmentally compliant formulations. Consequently, high-temperature-resistant rheological modifiers capable of enhancing dynamic shear stress (τ) while maintaining eco-compatibility have gained critical importance. Based on the requirements of such drilling, this study analyzed the rheological properties of nanostarch crystals(SNC) and explored their application prospects as flow pattern regulators for high temperature resistant drilling fluids in combination with the advantages of nanomaterials and starch materials. The results showed that nanostarch rheological property regulators are disc-shaped and strip-shaped. Compared with starch particles, the proportion of hydroxyl groups in crystal particles is higher, which is conducive to the adsorption and bridging performance of SNC particles. SNC have extremely strong thixotropy. When the concentration is 3%, the crystal suspension has good thixotropy, and when the concentration is doubled, the thixotropy is greatly enhanced, showing good suspension ability, and the sedimentation stability of the suspension is good, 48 hours without subsidence. It has a very positive impact on the drilling fluid system. Even after thermal aging at 150℃/16h (roller oven), it can improve the dynamic shear force of the drilling fluid system, reduce the filtration loss, and improve the thixotropic properties, that is, improve the suspension capacity of the drilling fluid system. Findings validate SNC effectively optimize shear thinning behavior, fluid loss control and solid sag resistance, demonstrating potential as advanced rheological modifiers for high-pressure/high-temperature (HTHP) drilling environments..

Keywords: drilling fluids; thermal stability; rheological property regulator; nanostarch crystals; thixotropy

1. Introduction

With the progressive depletion of conventional hydrocarbon resources, deep oil and gas exploitation has emerged as an industry priority[1]. Subsurface operations targeting these deep formations encounter complex challenges including elevated temperature-pressure conditions[2].Concurrently, tightening environmental regulations (per API Environmental Guidance Document) now mandate compliance with chroma specifications for drilling fluids in sensitive areas, rendering traditional additives such as lignosulfonates, asphaltic materials, humic acid derivatives, and sulfonated compounds operationally constrained. Modern drilling operations require fluid

 doi:10.20944/preprints202504.1790.v1

systems exhibiting optimal rheological characteristics, particularly maintaining effective cuttings transport capacity while preserving flowability[3]. Shear thinning properties have consequently become a critical fluid performance metric[4]. Among current rheology modifiers, xanthan gum biopolymers demonstrate field-proven effectiveness in conventional applications[5]. However, operational data confirm thermal degradation above 150°C , leading to viscosity reduction, shear strength deterioration, and elevated fluid loss.These constraints highlight the industry's critical need for environmentally acceptable rheology modifiers with enhanced temperature stability to optimize fluid rheological profiles in extreme downhole conditions[6].

In recent years, nanotechnology research has witnessed significant advancements in its drilling applications. With evolving drilling technologies,, extensive research has focused on the application of nanomaterials in drilling fluid. Li et al. investigated the effects of hydrophilic and hydrophobic nanosilica on rheological properties and fluid loss control in water-based drilling fluids[7]. Their results demonstrated that both nanosilica types effectively enhanced viscosity and shear stress under ambient conditions (25°C) and elevated temperatures (150°C). Zhong et al. developed crosslinked starch nanospheres (100-300 nm particle size) through reverse emulsion polymerization using methylenebisacrylamide[8]. This nanomaterial maintained drilling fluid rheological stability while achieving superior filtration control, and showed particular effectiveness in 150°C hydrocarbon well environments.. Djouonkep et al. engineered a thermally stable hybrid system combining polymer nanocomposites and bentonite through thermally-induced thickening mechanisms[9]. The system exhibited exceptional performance, retaining over 60% viscosity under extreme conditions (220°C with 20 wt% NaCl brine). Li et al. demonstrated that introducing cellulose nanocrystals (CNC) synergistically enhanced the rheological modification efficiency of functionalized cellulose derivatives in drilling fluids. This synergistic mechanism improves both low-shear viscosity and dynamic filtration control[10]. Lai et al. developed nano-reinforced thermoplastic corn starch composites incorporating nanobentonite and nanocellulose[11]. The composite's mechanical strength originated from nanobentonite's silicate layers, while nanocellulose enhanced flexibility via free volume modification in the polymer matrix. These findings validate that rationally designed nanomaterial combinations can generate multifunctional enhancements for drilling applications.

Starch exhibits semicrystalline characteristics[12]. Within its crystalline domain, the tightly packed and orderly aligned molecular chains create a densely structured matrix that hinders reagent penetration[13]. Industry research confirms that during gelatinization, the amorphous regions undergo preferential degradation, demonstrating superior thermal stability of the crystalline phase compared to disordered regions. This justifies the technical viability of employing starch crystalline domains as functional components in drilling fluid additives[14]. Post-gelatinization regeneration processes further enhance the material's performance characteristics:

Elevated crystalline stability with melting point maintained at ~150°C

Increased gelatinization onset temperature in regenerated starch

Structural integrity suitable for downhole thermal environments

These operational parameters validate the technical feasibility of deriving starch nanocrystals through gelatinization-ageing-regeneration protocols for high-temperature drilling fluid applications[15]. Building upon these findings, the present investigation explores synergistic formulations combining starch nanocrystals with polyanionic cellulose (PAC) to develop environmentally compliant rheological modifiers for advanced drilling fluid systems.

2. Materials and Methods

2.1 Materials

The main experimental materials included corn starch (dried at 55°C for 24 h with 200-mesh screening), sodium hydroxide (analytical grade), and concentrated sulfuric acid (>98% purity), all procured from Sinopharm Chemical Reagent Co., Ltd. Deionized water was laboratory-prepared.

 doi:10.20944/preprints202504.1790.v1

The experimental instruments include precision balance, model BS-224S, purchased from Beijing Sartorius Instrument Company. Intelligent magnetic stirrer, model ZNCL-GS, purchased from Qingdao Lanten Instrument Company. Three-mouth flask, purchased from scientific laboratory equipment store. Desktop high-speed centrifuge, model HHD-6, purchased from Hunan Kecheng Instrument Company. Digital speed control stirrer, model GS-2K, purchased from Decheng Hardware Store. Refrigerator, model BCD-220WMGR, purchased from Haier Group. Zeta potential and nanoparticle size analyzer, purchased from Brookhaven, USA.

2.2 Methods

2.2.1. Preparation of SNC

A beaker was charged with 456 mL deionized water. 94.55 mL of 98% sulfuric acid was slowly introduced along the beaker wall under continuous stirring to prepare the dilute acid solution. A separate solution containing 20 g NaOH dissolved in 500 mL deionized water was prepared.

A 66.67 g starch suspension was formulated with 150 mL deionized water and subjected to 80°C thermal conditioning for 30 min to achieve full polymer hydration. The gelatinized matrix underwent 5-day cryo-aging at 4°C to induce crystalline restructuring. 256 mL of 3.3M H_2SO_4 solution was introduced to initiate acid hydrolysis under controlled downhole-equivalent conditions (40°C/7-day, 200 RPM mechanical shear). Post-hydrolysis neutralization was conducted using 0.5M NaOH to pH 7.0±0.2, followed by primary solid-liquid separation via 8,000 RPM centrifugation (10 min) for pellet recovery. Three wash cycles were performed using 500 mL DI water/cycle with 30 min ambient shear dispersion and repeated 8,000 RPM centrifugation. Final purification involved low-speed clarification (600 RPM/10 min) to isolate supernatant nanoparticle suspension (Fig.1), succeeded by high-G force isolation (14,000 RPM/10 min) yielding drilling fluid-grade starch nanocrystals[16–19].

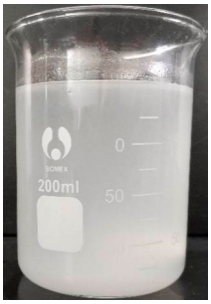

Figure 1. SNC suspension after centrifugation

2.2.2. Grain Size Distribution of SNC

The Brookhaven Omni Series Zeta potential/nanoparticle size analyzer was initialized with a 30-minute warmup protocol to achieve thermal stabilization. A 0.01% (w/v) aqueous dispersion was prepared by homogenizing starch nanocrystals in deionized water (DI-H_2O) through 30-minute magnetic shear conditioning at 800 RPM. Subsequently, 3 mL aliquots were loaded into quartz cuvettes for dynamic light scattering (DLS) characterization, with triplicate measurements conducted under Brownian motion parameters at 25°C ± 0.5°C ambient conditions.

2.2.3. Analysis of SNC by Transmission Electron Microscopy

Field-collected starch nanocrystals were dispersed in quantified aliquots of deionized (DI) water and subjected to 30-minute magnetic shear conditioning at 800 RPM to achieve a homogenized 0.01% (w/v) colloidal dispersion. Carbon-coated TEM grids were pretreated with lacey support films, onto which 3-5 μL samples were deposited via micropipette. Following solvent evaporation under controlled ambient conditions (25°C, 40% RH), crystalline morphology characterization was conducted using a field-emission transmission electron microscope operated at 200 kV acceleration

 doi:10.20944/preprints202504.1790.v1

voltage with Gatan Orius SC1000 CCD image capture, enabling sub-nanometer resolution imaging of the crystalline lattice structure[20].

2.2.4. Infrared Spectroscopy Analysis of SNC

NEXUS infrared spectrum analyzer was used to test the infrared spectrum of starch and SNC by KBr tabletting method. A suitable amount of sample was taken and mixed with dry potassium bromide powder. Generally, the mass ratio of sample to potassium bromide was about 1:100. The mixture was ground to a particle size of less than 2 μm. Then the ground sample was placed into a tabletting mold, pressed into transparent sheets on a tabletting machine, and tested on the sample holder of infrared spectrometer[21].

2.2.5. Viscosity Characteristics of SNC

SNC were prepared into suspensions with concentrations of 3%, 6% and 10%, respectively, and the viscosity of the suspensions at different shear rates was measured by Anton Paar rheometer to analyze their viscosity characteristics.

2.2.6. Thixotropy of SNC

Anton Paar rheometer was used to analyze the rheological characteristics of SNC with different concentrations, calculate the hysteresis loop area formed by the viscosity curve when the shear rate increased and decreased, compare and analyse the thixotropy of the suspension formed by SNC, and its adaptability in drilling fluid.

2.2.7. Effect of SNC on Rheological Properties and Fluid Loss Properties of Drilling Fluids

Pour the drilling fluid added with SNC into the sample cup and place it on the bracket of the instrument. Adjust the height so that the drilling fluid level is exactly at the measuring line of the rotary drum. Adjust the rotational speed of the viscometer to 600 r/min, and record the readings after the reading is stable. Use the same method to test the readings at 300 r/min , 200 r/min, 100 r/min, 6 r/min and 3 r/min in turn. Rotate at 600 r /min for 10 s and stand for 10 s, then record the maximum readings at 3 r/min. Rotate at 600 r/min for 10s and stand for 10 min, and then record the maximum readings at 3 r /min. Calculate the rheological performance parameters such as apparent viscosity (AV), plastic viscosity (PV), dynamic shear force (YP), dynamic plastic ratio (YP/PV) of the drilling fluid according to the following formula[22].

$$AV=\phi 600/2, \quad (1)$$

$$PV=AV-\varphi 300 \quad (2)$$

$$YP=AV-PV \quad (3)$$

2.2.8. Effect of SNC on the Filtration Performance of Drilling Fluid

Pour the drilling fluid added with SNC into the test container, cover with filter paper, place a graduated cylinder under the drain pipe, connect the pressure pipe, start timing while pressurizing, and measure the filtration loss at 6.9 Mpa for 30 minutes as the API filtration loss at room temperature and pressure[23].

3. Results and Discussion

3.1 Particle Size Distribution

According to the established preparation protocol for SNC, final SNC products were successfully synthesized. Subsequent characterization employing a 0.01% SNC suspension was

 doi:10.20944/preprints202504.1790.v1

conducted to validate particle size distribution and confirm the nano-scale dimensions of the obtained material.

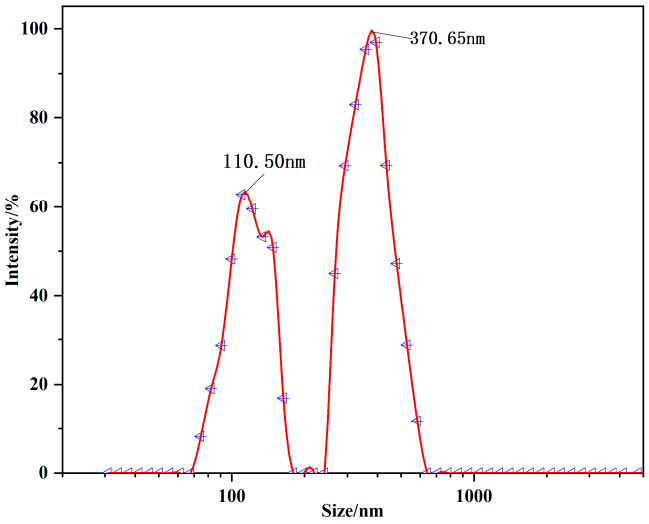

Figure 2. Particle size distribution curve of SNC

The synthesis of SNC was achieved through acid hydrolysis. However, this process exhibits non-directional etching characteristics, whereby the acid may randomly attack starch particles from multiple crystallographic orientations, resulting in irregular morphological features in the final product. As per the operational principles of dynamic light scattering instrumentation (e.g., Malvern Zetasizer Nano ZSP), the measured particle size corresponds to the hydrodynamic diameter - defined as the equivalent spherical diameter that would diffuse at an identical rate to the target particle in suspension. According to the particle size data obtained in Fig. 2, the SNC obtained by acid hydrolysis has two main particle size peaks, 110.50 nm and 370.65 nm respectively. Based on the calculation principle of the relationship between the number of particles and the size distribution, it can be known that the number of particles with a particle size of about 110.50 nm accounts for a higher proportion[24]. According to the above analysis, the minimum size of SNC may be several nanometers, tens of nanometers, or hundreds of nanometers. From a rheological modification perspective, particle geometry critically impacts performance: elongated or structurally anisotropic particles demonstrate enhanced capability for forming three-dimensional network architectures, thereby optimizing drilling fluid rheology. To conclusively validate these morphological hypotheses, transmission electron microscopy (TEM) characterizations were essential for direct nanoscale visualization[25].

3.2 Transmission Electron Microscope

Transmission electron microscopy (TEM) serves as an indispensable characterization tool for direct visualization of nanoparticle morphologies. This analytical modality achieves atomic-level resolution to resolve critical structural parameters including crystalline dimensions, geometric configurations, and surface topography - essential data for comprehensive nanomaterial analysis.

 doi:10.20944/preprints202504.1790.v1

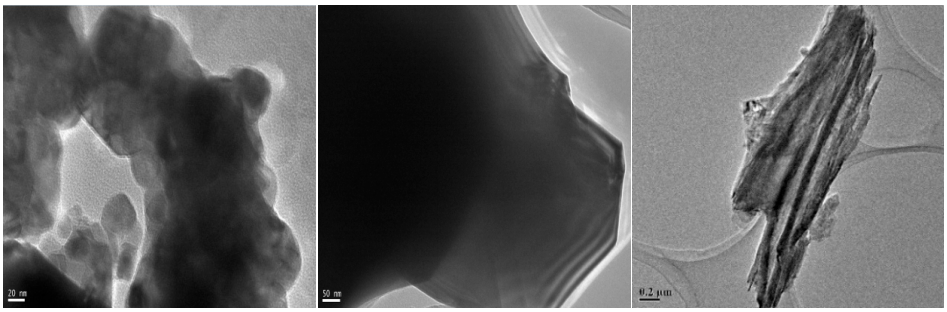

Figure 3. Transmission electron microscopy of starch nanocrystals

Structural characterization reveals that acidolyzed SNC exhibit dual morphological configurations: disc-shaped and strip-shaped, with monocrystalline domains measuring approximately 50 nm in lateral dimension. TEM micrographs reveal distinct morphological classifications, while partial nanostarch particulates demonstrate interparticle agglomeration via hydrogen-bonded stacking, discrete crystalline units maintain colloidal stability through electrostatic repulsion(Figure 1a). The second figure shows that the crystal edges are acute polygons, and obvious layered structures can be observed, which also increases the adsorbable area of the crystals[26]. The third figure shows that the single SNC particles are elongated, which is conducive to better bridging in the drilling fluid system, thus enhancing the thixotropy of the drilling fluid system macroscopically. When the drilling fluid stops flowing, the grid structure formed can make the rock debris in it not easy to settle. However, when the drilling fluid starts to flow, the grid structure can be quickly destroyed due to the small particles of SNC, so that the drilling fluid system can flow better[27].

3.3 Infrared Broad Spectrum

Fourier-transform infrared (FTIR) spectroscopy provides critical functional group analysis through characteristic molecular vibration fingerprints. Comparative evaluation of FTIR spectra between native starch granules and acid-hydrolyzed SNC reveals hydrolysis-induced compositional alterations. As evidenced by literature, acid hydrolysis mediates hydroxyl group enrichment in starch crystallites[28]. Figure 4 demonstrates near-identical FTIR signatures for both materials, yet shows hydroxyl (-OH) stretching vibration migration (3200-3500 cm^{-1}) with 1.06% peak intensity elevation in nanostarch specimens, confirming enhanced hydroxylation.

This hydroxyl group proliferation strengthens intramolecular hydrogen bonding networks , significantly improving drilling fluid's transient gelation kinetics. Specifically, accelerated 3D network lattice formation during fluid-static transitions achieves superior cuttings suspension while maintaining favorable shear-thinning responsiveness[29]. Concurrently, intensified absorbance at 1155.17 cm^{-1} (C-O-S stretching) confirms sulfonic acid group incorporation during hydrolysis[30].

 doi:10.20944/preprints202504.1790.v1

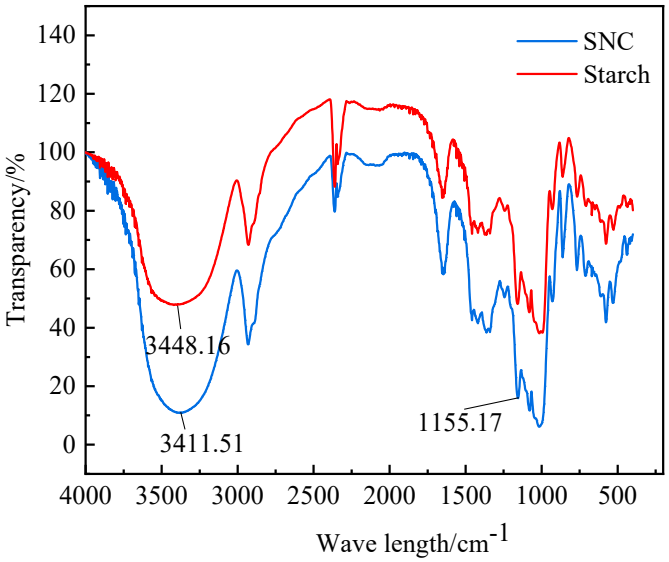

Figure 4. Infrared spectra of starch nanocrystals and starch

3.4 Viscosity Characteristics

When the shear rate increases, the entanglement structure between molecular chains is destroyed, and the molecular chains are oriented, so that the relative flow resistance between chains decreases, resulting in a decrease in viscosity[31]. As can be seen from the test results, the viscosity characteristics of SNC are similar to those of polymers.

SNC suspensions were prepared at varying mass concentrations (3-10 wt%) and subjected to rheological characterization using an Anton Paar MCR 302 rheometer with concentric cylinder geometry (CC27), as illustrated in Figure 5. The flow curves demonstrate characteristic shear-thinning behavior, where apparent viscosity decreases exponentially with increasing shear rate (0.01-1000 s^{-1}). This pseudoplastic response aligns with conventional polysaccharide-based drilling fluid additives, where viscosity reduction originates from the breakdown of physical crosslinking networks formed through[31].When the shear rate increases, the entanglement structure between molecular chains is destroyed, and the molecular chains are oriented, so that the relative flow resistance between chains decreases, resulting in a decrease in viscosity. The viscosity-shear rate profile of SNC shows striking parallels to synthetic polymer solutions, confirming their potential as sustainable rheology modifiers via analogous shear-dependent viscoelastic mechanisms.

For the 3 wt% SNC suspension, viscosity stabilization was observed at shear rates exceeding 200 s^{-1}. Under high-shear conditions, polymer chains achieve full molecular alignment, rendering further shear rate increases minimally impactful on chain orientation or conformational adjustments, thereby establishing steady-state hydrodynamic equilibrium with stabilized viscosity[32]. This phenomenon implies that during drilling fluid circulation, viscosity invariability can be maintained once critical flow velocity thresholds are reached, offering theoretical foundations for designing constant-rheology drilling fluid systems through controlled nanostarch crystallization engineering.

 doi:10.20944/preprints202504.1790.v1

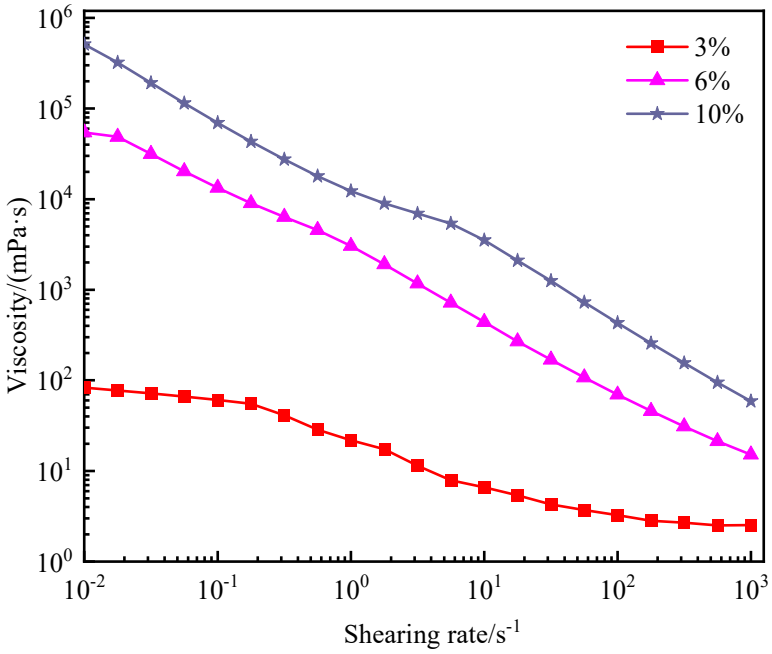

Figure 5. Viscosity curves of starch nanocrystalline suspensions with different concentrations

3.5 Thixotropy of SNC

As the shear stress increases, the original structure between the particles in the test fluid is destroyed by the shear force, causing the viscosity of the fluid to decrease. When the shear force stops, the structure between the particles gradually recovers due to the existence of the interaction force. Since the structural recovery takes a certain amount of time, when the shear stress increases first and then decreases, the two viscosity curves will not overlap, forming a curve that cannot be closed. For drilling fluid, its thixotropy refers to the property that the drilling fluid becomes thinner when stirred and becomes thicker after stirring stops . A drilling fluid system with good thixotropy is very important in the drilling process. It can not only reduce the resistance of the drilling fluid during circulation, but also quickly restore the structure to suspend the cuttings when the circulation stops. Therefore, the thixotropy of SNC is an important part of its application as a rheology modifier in drilling fluid.

Anton Paar rheometer was used to analyze the rheological characteristics of SNC with different concentrations, calculate the area of hysteresis loop formed by the viscosity curve when the shear rate increases and decreases, compare and evaluate the thixotropy of the suspension formed by SNC, and analyze its adaptability in drilling fluid. The experimental results are shown in Fig. 6. The area between the viscosity curve of the shear rate increase and the shear rate decrease of the SNC suspension with different concentrations calculated according to the data in the figure is shown in Table 1.

 doi:10.20944/preprints202504.1790.v1

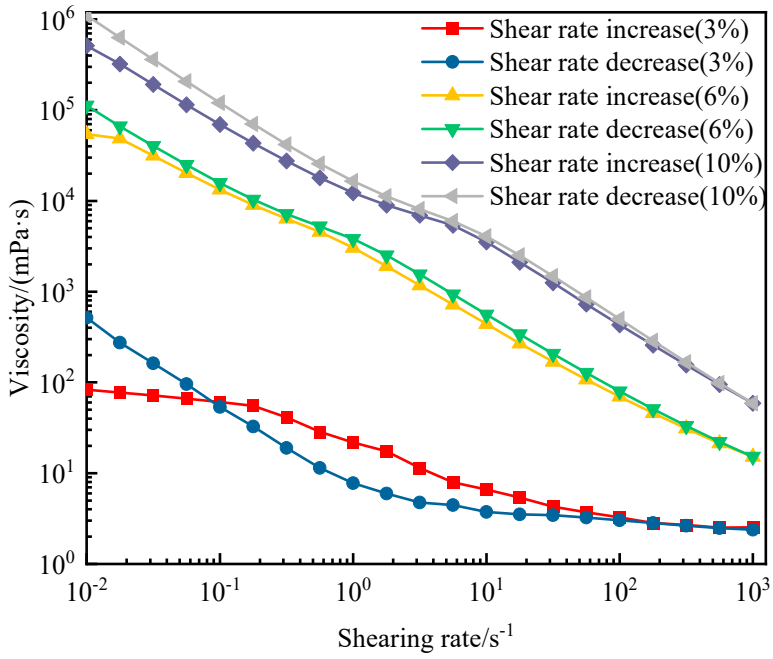

Figure 6. Viscosity curves of SNC suspensions

Table 1 Area of the curve between SNC suspensions with different concentrations

Concentration of nanometer starch crystals/%	3	6	10
Curve area	199.12	8802	60151

According to the rheological analysis results (Table 1), the hysteresis loop area between the ascending and descending shear rate viscosity curves of nanostarch crystal-modified drilling fluid expands with increased additive concentration (3%, 6%, 10%), demonstrating enhanced thixotropic behavior. This phenomenon arises from the particle interaction dynamics: at lower concentrations (3%), reduced interparticle attractive forces (Van der Waals forces and hydrogen bonding) and predominant Brownian motion result in slower structural regeneration. With concentration escalation, higher particle density per unit volume promotes interparticle contact frequency and hydrogen bond network formation, thereby accelerating gel strength rebuild rate[33]. Notably, at 6% and 10% concentrations, the descending shear rate viscosity significantly exceeds ascending values, indicating shear-induced particle orientation alignment that enhances adsorption sites and suspension capacity. Even at 3% concentration, when shear rate drops below 0.1 s^{-1}, the fluid exhibits superior viscosity retention during shear reduction phases, confirming concentration-dependent structural recovery capacity characteristic of thixotropic drilling fluids

3.6 Settling Stability of Suspension

The high specific surface area of nanomaterials promotes interparticle adsorption and aggregation, making the investigation of sedimentation stability in SNC suspensions crucial for their application in drilling fluid systems[34]. 0.5 wt% and 1.0% SNC suspensions were prepared and subjected to static settling observation in sample vials, with experimental results displayed in Figure 7. This evaluation methodology directly reflects the colloidal stability and anti-settling properties of nanoparticles under quiescent conditions – key performance indicators for drilling fluid additives requiring prolonged suspension of weighting materials and cuttings.

 doi:10.20944/preprints202504.1790.v1

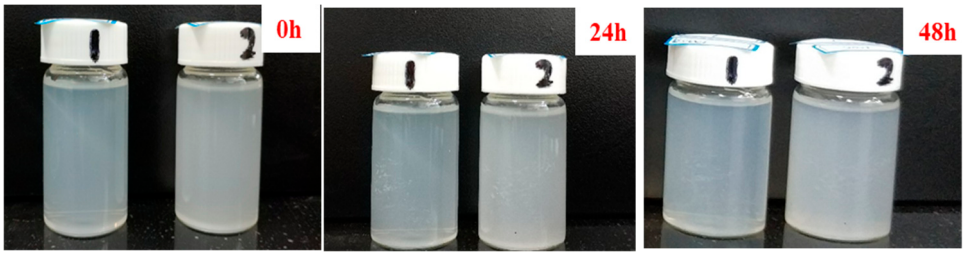

Figure 7. Sedimentation stability of SNC suspensions (1)0.5% (2) 1.0%

As shown in Figure 7, the SNC suspensions exhibited no sedimentation after 48 hours of static settling. Zeta potential analysis revealed a value of -37.62 mV(0.5%) and -31.21mV(1.0%), with the absolute magnitude exceeding the critical threshold of 30 mV. This strongly indicates superior colloidal stability in the SNC drilling fluid system.

The observed high stability aligns with established colloidal theories:

Electrostatic stabilization mechanism: The zeta potential magnitude significantly surpasses the ±30 mV stability threshold for aqueous nanoparticle dispersions, suggesting strong electrostatic repulsion between particles that prevents aggregation[35].

DLVO theory validation: The large negative surface charge creates sufficient electrical double-layer repulsion to overcome van der Waals attractive forces, maintaining system homogeneity under static conditions[36].

Drilling fluid applicability: Such stability parameters meet the operational requirements for weighting agent suspension and wellbore cleaning in drilling operations, where prolonged particle suspension capability is crucial.

This stability profile demonstrates the SNC' potential as a sustainable additive for designing advanced drilling fluids with enhanced suspension characteristics and prolonged shelf stability.

Table 2 Zeta potential of SNC suspensions with different concentrations

Concentration/%	Zeta potential/mV
0.3	-42.25
0.5	-37.62
1.0	-31.21
2.0	-30.84

The formulated SNC suspensions with varying concentrations were evaluated for sedimentation stability patterns through Zeta potential measurements (Table 2). The experimental data revealed a concentration-dependent Zeta potential attenuation trend, where increasing SNC concentration from 0.5% to 2% reduced the absolute Zeta potential value from -42.25 mV to -30.84 mV. Notably, at 2% concentration, the suspension maintained a Zeta potential magnitude of 30.84 mV, demonstrating persistent colloidal stability.

3.7 Effect on Rheological Properties of Drilling Fluids

3.7.1. The Impact of SNC on the Rheological Profile and Fluid Loss Control Performance of Water-based Drilling Fluids

A series of drilling fluid formulations incorporating SNC at varying concentrations were prepared using a base mud of 4 wt% bentonite + 0.5 wt% high-temperature stabilizer. Rheological parameters (yield point, plastic viscosity, YP/PV ratio) and filtration loss were evaluated befor and after thermal aging (150°C/16 hours). Subsequent analysis (Table 3) revealed: At low SNC

 doi:10.20944/preprints202504.1790.v1

concentrations (0.5 wt%), no alterations in rheological profiles were observed. Progressive SNC addition induced concentration dependent improvements measurable increases in yield point (100-250% enhancement), elevated YP/PV ratios (49-57.5% transition), and reduced filtration loss volumes (17.9-28.8% reduction). With the addition of SNC, the thickness of mud cake obtained by the filtration loss measurement experiment is reduced, which is conducive to the formation of thin and tough mud cake. These trends conclusively demonstrate SNC's dual functionality as a yield point enhancer and filtration control agent, while maintaining thermal stability under designated HTHP conditions.

Table 3 Evaluation of rheological and filtration properties of different experimental mud

Concentration of SNC/%	Test conditions	AV /(mPa·s)	PV /(mPa·s)	YP/Pa	YP/PV	FL_{API} /mL	pH	H_k /mm
0	Before rolling	5	3	2	0.67	28	10	1
	After rolling	3.5	2.5	1	0.40	34	8	1
0.5	Before rolling	5	3	2	0.67	27.8	10	0.5
	After hot rolling	3.5	2.5	1	0.40	32.4	9	0.5
1.0	Before rolling	8	4	4	1.00	23.0	9	0.5
	After rolling	6.5	4	2.5	0.63	24.2	8	0.5
1.5	Before rolling	9	4	5	1.25	22.6	9	0.5
	After rolling	7	4	3	0.75	23.4	8	0.5

3.7.2 Effect of SNC on Thixotropy of Drilling Fluids

Different concentrations of SNC were added to the drilling fluid, and the rheological characteristics were analyzed by testing the viscosity change during the increase and decrease of the shear rate of the drilling fluid. According to Figures 8 to 10, the area between the viscosity curves of the drilling fluid with the increase and decrease of shear rate before and after adding different concentrations of SNC was calculated, and the influence of SNC on the thixotropy of the drilling fluid was compared by the area size (Table 4). It can be seen that a small amount of SNC can enhance the thixotropic property of the drilling fluid. With the increase of the concentration of SNC, the thixotropicity of the drilling fluid was enhanced. When the concentration was 3% and 6%, the viscosity of the drilling fluid when the shear rate decreased was greater than that when the shear rate increased, indicating that the suspension showed stronger suspension ability after shearing.

SNC was incorporated at varying concentrations into the drilling fluid, and the viscosity changes of the fluid during shear rate ramping (increasing and decreasing cycles) were measured to analyze its rheological properties before and after hot rolling. Based on Figures 8 to 10, the area between the curves during shear rate ramping and declining was calculated for the drilling fluid with and without SNC. This hysteresis loop area, quantified in Table 4, was used to evaluate the impact of SNC on the thixotropic behavior of the fluid. The results indicate that even low concentrations of SNC significantly enhanced the thixotropy of the bentonite-based drilling fluid. As the starch concentration increased, the thixotropic properties of the fluid improved further. At concentrations of 3% and 6%, the viscosity during shear rate decline exceeded that during shear rate ramp-up, demonstrating that the suspension exhibited stronger structural recovery and enhanced particle-suspending capability after shear stress application.

Table 4 Area of the curve between SNC suspensions with different concentrations

 doi:10.20944/preprints202504.1790.v1

Drilling fluid	Base mud	Base mud + 0.1% SNC	Base mud + 1% SNC	Base mud + 3% SNC	Base mud + 6% SNC
Curve area	153	232	2647	11463	24928

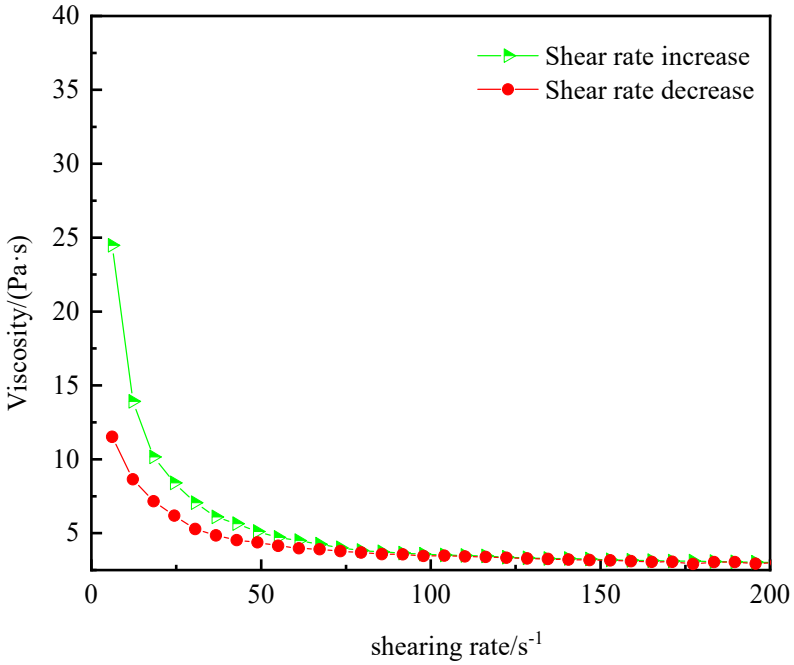

Figure 8. Viscosity curve of bentonite base mud

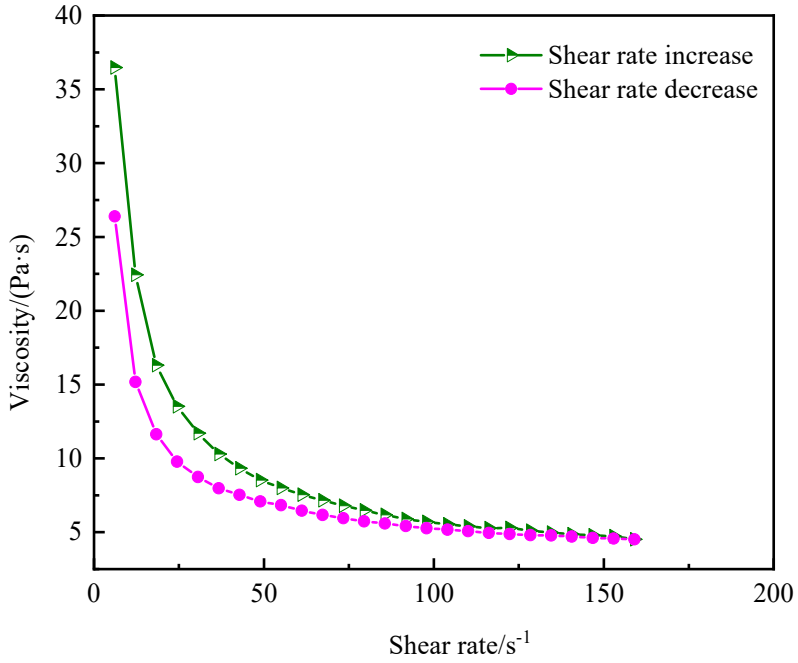

Figure 9. Viscosity change curve of bentonite base mud under 0.1% SNC dosage

When the concentration of SNC is 1%, during the process of decreasing shear rate, when the shear rate decreases to below 0.02 s-1, the viscosity of the SNC suspension is higher than the viscosity when the shear rate increases. When the concentration is 3% and 6%, the viscosity during the process

 doi:10.20944/preprints202504.1790.v1

of decreasing shear rate is always higher than the viscosity when the shear rate increases, indicating that the suspension exhibits a stronger suspension ability (Figure 10).

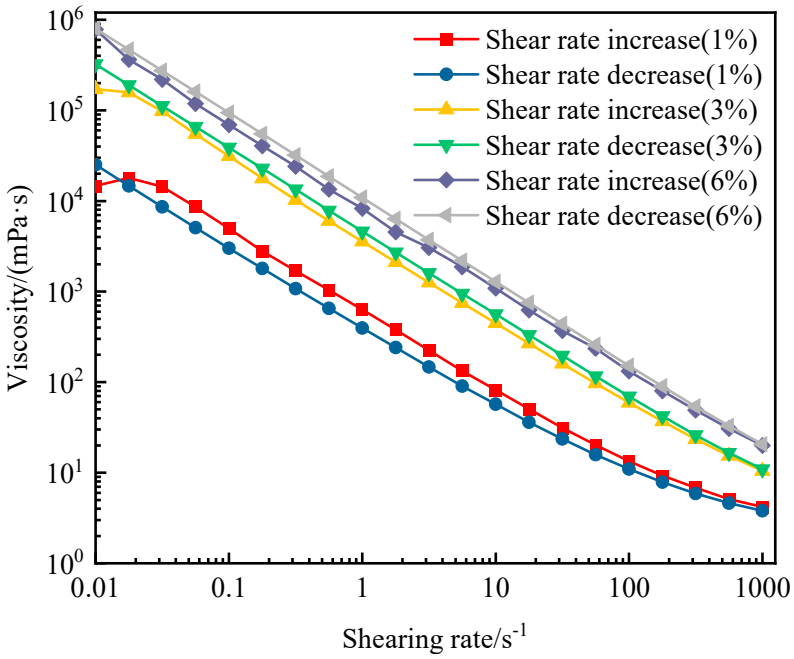

Figure 10. Viscosity change curve of bentonite base mud under different SNC dosage

3.8 Structural Reconstruction Performance

By designing different shear rates (0.1 s-1, 1000 s-1and 0.1 s-1) to cyclically shear different dispersion systems, and combining the recovery of the suspension viscosity when the shear rate changes from high to low, the reconstruction performance of the grid structure can be analyzed. SNC were added to deionized water to prepare suspensions of different concentrations, and their structural reconstruction performance was tested (Figure 11).

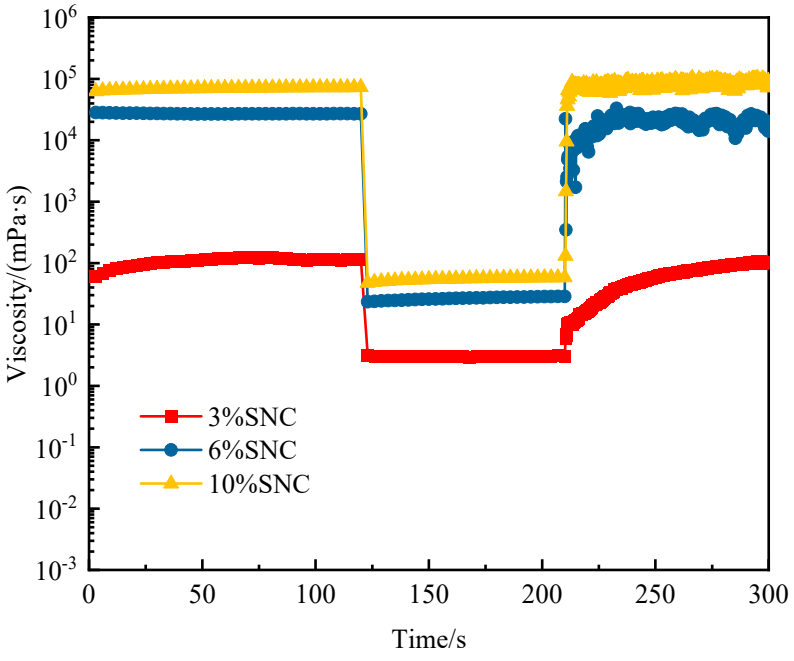

Figure 11. Structural reconstruction performance of SNC suspension

Experimental observations demonstrate that SNC suspensions at varying concentrations exhibit structural reconstruction capability post-shear degradation, with reformed three-dimensional

 doi:10.20944/preprints202504.1790.v1

networks approximating the initial structural integrity. Increasing SNC concentration accelerated structural recovery kinetics, as evidenced by the 3%–6% SNC dosage range: the viscosity augmentation rate and structural reformation speed escalated markedly, correlating with elevated particle density per unit volume. This intensified interparticle proximity facilitates rapid hydrogen bond reconfiguration, thereby enhancing network re-establishment efficiency. Such accelerated percolating network regeneration critically improves drilling fluid cuttings suspension performance. Notably, while 6% SNC suspensions achieved faster structural recovery than lower concentrations, comparative analysis reveals prolonged viscosity stabilization periods and amplified fluctuation magnitudes relative to 10% SNC formulations.

4. Conclusions

SNC were synthesized via acid hydrolysis and systematically characterized to evaluate their applicability in petroleum drilling fluids. The synthesized SNCs exhibited a discoidal morphology with axial elongation (mean particle size: 314.36 nm) and demonstrated enhanced hydroxyl group density compared to native starch particles, thereby optimizing their adsorption capacity and bridging functionality. Rheological characterization revealed polymer-like shear-thinning behavior in SNC suspensions. Notably, 3 wt% SNC suspensions maintained viscosity invariance at elevated shear rates (≥300 s^{-1}), demonstrating potential utility in constant-rheology drilling fluid formulations. SNC also had strong thixotropy. When the concentration was 3%, the crystal suspension had good thixotropy, and when the concentration was doubled, the thixotropy was greatly enhanced, showing good suspension ability. Moreover, the suspension had good settling stability, and did not settle for 48 hours. SNC had a very positive effect on the drilling fluid system. It could improve the dynamic shear force of the drilling fluid system and reduce the filtration loss of the drilling fluid system, i.e., improve the suspension ability of the drilling fluid. SNC shows excellent capability for improving rheological properties of drilling fluids.

Author Contributions: "Conceptualization, Guowei Zhou; methodology, Guowei Zhou and Xin Zhang; validation, Lixin Wen; investigation, Rugang Yao; data curation, Zhengsong Qiu; writing—original draft preparation, Guowei Zhou; writing—review and editing, Zhengsong Qiu. All authors have read and agreed to the published version of the manuscript."

Acknowledgments: This research is thanks to the postdoctoral workstation of CNPC Greatwall Drilling Company, the postdoctoral research station of China University of Petroleum (East China), and the support of CNPC Greatwall Drilling Company's project "Research on new materials of water-based drilling fluid system and core treatment agent resistant to 200℃ high temperature".

References

1. Wang, S. Y., Sun, Z. H., Zhu, Q., Cao, X. Q., Feng, Y. J., Yin, H. Y. In Situ Generated Hydrogels Exhibiting Simultaneous High-Temperature and High-Salinity Resistance for Deep Hydrocarbon Reservoir Exploitation. INDUSTRIAL & ENGINEERING CHEMISTRY RESEARCH. 2024, 63(43), 18263-18278.
2. Martin, A. Nourian, M. B., Nasr, G. G. Innovative drilling fluid containing sand grafted with a cationic surfactant capable of drilling high pressure and high temperature geothermal and petroleum wells. Geoenergy Science and Engineering. 2024, 237, 212767.
3. Mahmoud, H., Alhajabdalla, M., Mohammed, A., Nasser, M. S., Hussein, I. A., Ahmed, R., Karami, H. Pilot-scale study on the suspension of drill cuttings: Effect of fiber and fluid characteristics. JOURNAL OF NATURAL GAS SCIENCE AND ENGINEERING. 2022, 101, 104531.
4. Huang, F. Y., Chen, L. F., Sheng, W. W., Shang, X. X., Zhang, Z. N. Thixotropy and gelation characteristics of thermosensitive polymer nanofluids at high temperature. Colloids and Surfaces A: Physicochemical and Engineering Aspects. 2025, 711, 136340.
5. Al-Ziyadi, H., Pandian, S., Verma, A. Utilization of silica microfiber to enhance the rheological properties and fluid loss control of water-based drilling fluids. ENERGY SOURCES PART A-RECOVERY UTILIZATION AND ENVIRONMENTAL EFFECTS. 2025, 47(1), 5027-5040.

 doi:10.20944/preprints202504.1790.v1

6. Walsh, John, Ramesh, S. Fit-for-Purpose Water Treatment in Permian Shale – Field Data, Lab Data and Comprehensive Overview. SPE Annual Technical Conference and Exhibition, September 2018. Dallas, Texas, USA. 191529-MS.
7. Li, X. L., Kai, W., Yingjun, L., Xiulun, S., Hehai, Z., Jianghao, P., Shangli, J., Ming, D. Compatibility and efficiency of hydrophilic/hydrophobic nano silica as rheological modifiers and fluid loss reducers in water-based drilling fluids. Geoenergy Science and Engineering. 2024(234), 212628
8. Hanyi, Z., Xiangzheng, K., Siqi, C., Brian, P. G., Zhengsong, Q. Preparation, characterization and filtration control properties of crosslinked starch nanospheres in water-based drilling fluids. Journal of Molecular Liquids. 2021, 325, 115221.
9. Lesly, D. W., Binqiang, X., Huaizhi, T., Jindong, C., Lvyan, Z., Naomie, B. S., Alain P. T., Lin Z. Thermo-thickening/amphoteric polymer nanocomposite incorporating vinyl-functionalized nano-silica as a viscosifier for high-salt and ultra-high temperature water-based drilling fluids. Journal of Molecular Liquids. 2024(404), 124866.
10. Meichun, L., Qinglin, W., Kunlin, S., Yan, Q., Yiqiang, W. Cellulose Nanoparticles as Modifiers for Rheology and Fluid Loss in Bentonite Water-based Fluids. Applied Materials &Interfaces. 2015, 7, 5006-5016.
11. Di, S. L., Azlin, F. O., Sinar, A. A., Ismai, I., Midhat, N. A., Mariatti, J. Toughening mechanism of thermoplastic starch nano-biocomposite with the hybrid of nanocellulose /nanobentonite. Polymer. 2023, 274, 125876.
12. Duan, H. Crystalline structure of starch granules. Science and Technology, 2009, 154(15), 106.
13. Vamadevan, V., Bertoft, E. Structure-function relationships of starch components. STARCH-STARKE. 2015, 67(1-2), 55-68.
14. Zhang, L. M., Chen, D. Q. Structure-property relationships of new water-soluble grafted starches with amphoteric character. MACROMOLECULAR MATERIALS AND ENGINEERING. 2003, 288(3), 252-258.
15. Xuxu, L., Ruonan, H., Dan, W., Dapeng, L., Tao, Y., Shanbai, X., Qilin, H. Micro- and nano-sized starch to inhibit gel deterioration and myofibrillar protein strands bunching by molecular interactions under multiple freeze-thaw cycles. Food Hydrocolloids. 2024, 152, 109890.
16. Raozhen, Z., Xiangli, K., Yajuan, W., Yan, H., Shanggui, D., Xuechen, Z., Dan, Q. Isolation and characterization of natural nano starch from amaranth starch. International Journal of Biological Macromolecules. 2024, 260(1), 129525.
17. Tao, L., Kun, Q., Jiayao, F., Ziqi, Q., Long, Y., Jinjun, W., Wei, D. Nano-based smart pesticide formulations utilizing starch nanocrystals: Achieving high stability and extended effective duration. Industrial Crops & Products. 2024, 214, 118470.
18. Suman, K., Baljeet, S., Yadav, R. Y. Characterization of acid hydrolysis based nano-converted mung bean (*Vigna radiata L.*) starch for morphological, rheological and thermal properties. International Journal of Biological Macromolecules. 2022, 211, 450-459.
19. Dagmara, B. nanostarch for food applications obtained by hydrolysis and ultrasonication methods. Food Chemistry. 2023, 402, 134489.
20. Hanyi, Z., Shusen, L., Daqi, L., Junbin, J., Changzhi, C., Tingbo, M., Zhengsong, Q., Weian, H. Carbon microspheres prepared from soluble starch hydrothermal carbonization for extending thermal stability of water-based drilling fluid. International Journal of Biological Macromolecules. 2024, 282(6), 137391.
21. Cao, R. G., Gao, Y., Wang, L., Li, C. M., Wang, Z. Y., Li, Y. T., Qiu, J. Mechanistic insights into starch behavior and starch-protein interactions in whole grain oat flour: Structural and functional modifications by steam explosion treatment. INTERNATIONAL JOURNAL OF BIOLOGICAL MACROMOLECULES. 2025, 307(2), 142058.
22. Zhu, W. X., Luo, Y. H., Li, H. D., Gong, Y. F. Application of a Novel Temperature-Sensitive Polymer PNA-SiO2 as a Rheological Agent in Geothermal Drilling. ACS OMEGA. 2025, DOI10.1021/acsomega.4c09819.
23. Arain, A. H., Ridha, S. Effect of multifunctional boron nitride nanoparticles on the performance of oil-based drilling fluids in high-temperature unconventional formation drilling. GEOENERGY SCIENCE AND ENGINEERING. 2025, 247, 213722.

 doi:10.20944/preprints202504.1790.v1

24. Fedoseev, V. B., Shishulin, A. V. On the Size Distribution of Dispersed Fractal Particles. THEORETICAL AND MATHEMATICAL PHYSICS. 2021, 66, 34-40.
25. Tongtong, Z., Liang, Z., Ruixuan, Z., Qiannan, L., Wei, L., Honghai, H. Effects of particle size distribution of potato starch granules on rheological properties of model dough underwent multiple freezing-thawing cycles. Food Research International. 2022, 156, 111112.
26. Wenxian, G., Xinxin, M., Chao, R., Hongtao, W., Wei, L. Formation of crystalline multimetallic layered double hydroxide precipitates during uptake of Co, Ni, and Zn onto γ-alumina: Evidence from EXAFS, XRD, and TEM. Chemosphere. 2022, 307, 136055.
27. Seid, R. F., Hadis, R., Elham, A., Seid, M. J. Morphology and microstructural analysis of bioactive-loaded micro/nanocarriers via microscopy techniques; CLSM/SEM/TEM/AFM. Advances in Colloid and Interface Science. 2020, 280, 102166.
28. Gonzalez, A., Wang, Y. J. Effects of acid hydrolysis level prior to heat-moisture treatment on properties of starches with different crystalline polymorphs. LWT-FOOD SCIENCE AND TECHNOLOGY. 2023, 187, 115302.
29. Zhao, J., Chen, R., Cheng, D. M., Yang, X. Y., Zhang, H., Zheng, J. P., Hu, R. F. Extremely Ultrahigh Stretchable Starch-Based Hydrogels with Continuous Hydrogen Bonding. Advanced Functional Materials. 2025, 35(8).
30. Li, Y. J. Study on characteristics of fermented rice flour and its starch [D]. Zhengzhou: Henan University of Technology, 2010.
31. Joseph, J. B., Rothstein, J P. Recovery dynamics and polymer scission in capillary breakup extensional rheometry. JOURNAL OF NON-NEWTONIAN FLUID MECHANICS. 2025, 337, 105396.
32. Guancheng, J., He, S., Yinbo, H. The biodiesel-based flat-rheology drilling fluid system. PETROLEUM EXPLORATION AND DEVELOPMENT. 2022, 49(1), 200-210.
33. Vanitha, N., Revathi, T., Jeyalakshmi, R. Influence on Rheology and Microstructure of Nanosilica and Modified Polycarboxylate in Water-Glass-Activated Fly Ash/Ground Granulated Blast Furnace Slag Geopolymers. CHEMISTRYSELECT. 2023, 8(1), e202203491.
34. Haridas, H., Kontopoulou, M. Effect of specific surface area on the rheological properties of graphene nanoplatelet/poly(ethylene oxide) composites. JOURNAL OF RHEOLOGY. 2023, 67(3), 601-619.
35. Seong, H. J., Kim, G. N., Jeon, J. H., Jeong, H. M., Noh, J. P., Kim, Y. J., Kim, H. J., Huh, S. C. Experimental study on characteristics of grinded graphene nanofluids with surfactants. Materials. 2018, 11, 950.
36. Graves, J. E., Latvyte, E., Greenwood, A., Emekwuru, N. G. Ultrasonic preparation, stability and thermal ˙conductivity of a capped copper-methanol nanofluid. Ultrasonics Sonochemistry. 2019, 55, 25–31.